SACOMAR

Technologies for Safe and Controlled Martian Entry

SPA.2010.3.2-04

EU-Russia Cooperation for Strengthening Space Foundations (SICA)

Re-entry Technologies and Tools

Theme 9 - Space
Activity 9.3 - Cross-Cutting-Activities
Area 9.3.2 - International Cooperation

Deliverable Reference Number: D 5.6
Deliverable Title:

Results of the Experimental Study in the L2K Facility

Due date of deliverable: 31st October 2011

Actual submission date: 30th November 2011

Start date of project: 20th January 2011

Duration: 18 months

Organisation name of lead contractor for this deliverable: DLR, AS-HY

Revision #: 0

Project co-funded by the European Commission within the seventh Framework Programme		
Dissemination Level		
PU	Public	X
PP	Restricted to other programme participants (including the Commission	
RE	Restricted to a group specified by the consortium (including the Commission	
CO	Confidential, only for members of the consortium (including the Commission Services)	

APPROVAL

Title	issue	revision
Results of the Experimental Study in the L2K Facility	1	0

Author(s)	date
B. Esser, U. Koch, A. Gülhan	30.11.2011

Approved by	date
A. Gülhan	30.11.2011

Table of Contents

List of figures

List of tables

Nomenclature

Abbreviations

DLAS	Diode Laser Absorption Spectroscopy
DLR	German Aerospace Center
HFM	Heat Flux Microsensor
L2K	DLR's 1.4 MW arc heated facility in Cologne
LIF	Laser Induced Fluorescence
WP	Work Package

Symbols

D	Diameter
p	Pressure
r	Radius
x	Axial position

Subscripts

e	edge

1   Executive summary

1.1   Scope of the deliverable

A fundamental prerequisite for reliable application of CFD simulation to hypersonic planetary entry flows is a realistic thermochemical model of the planet's atmosphere. Although computational power has grown by orders of magnitudes within the last years, a CFD simulation code that is applicable to 3D configurations is still far away from being able to account for all microscopic effects that have influence on the macroscopic behaviour of a gas at high temperatures. The transfer from microscopic to macroscopic scale is performed by thermochemical modelling. Therefore, in advance to a CFD validation a reliable validation of the implemented thermochemical model has to be performed.

With regard to Earth atmosphere there is a huge experience accumulated and there has been a large number of space missions as well as flight and ground experiments that can be used for model validation. Compared to Earth atmosphere the thermochemical modelling of Martian atmosphere is more complex and covers a wider range of thermodynamical states due to several aspects:

The main objectives of the SACOMAR study are the improvement of experimental and numerical tools to study the aerothermodynamic problems of Martian entry, the achievement of a better understanding of physical phenomena and the creation of a data base. The main objective of the experimental activities in SACOMAR is to provide reliable measured reference data for the validation of thermochemical models of Martian atmosphere and their application within numerical simulation tools. Herein, the principal focus is set to a better understanding of thermochemical relaxation phenomena and its influence on surface heating. Test conditions, model geometries and measurement techniques had been specified in the SACOMAR test plan [1] based on the operational regimes of the individual test facilities and the necessities of future missions to Mars which are exemplarily deduced from the EXOMARS mission.

One of the high enthalpy facilities is the arc-heated facility L2K. In this document the test campaign performed in L2K is described in detail. In particular, it includes a description of the experimental setup, the applied measurement techniques, test procedures and all results obtained from the measurements.

1.2   Results

Measurements in L2K were performed at two different test conditions at different enthalpy levels which had been specified in the SACOMAR test plan. The first test condition FC-1 is characterized by a high total enthalpy of 13.8 MJ/kg. The enthalpy level of the second test condition FC-2 is considerably lower at 9.0 MJ/kg. In a first step, compliance to the specified test condition was demonstrated by Pitot pressure measurements. Additionally, radial homogeneity of the flow field was proved by Pitot pressure profiles.

In the first subset of tests, the cold wall heat flux in the stagnation point of two flat-faced cylinder models was measured with different techniques, i.e. a so-called heat flux microsensor (HFM) and a slug calorimeter made of stainless steel. It was found that the slug calorimeter systematically provided lower heat fluxes when compared to the HFM measurements. Taking HFM as reference the reduction was nearly constant between 28% and 36% and can be related to the different surface catalycity. While the surface of the HFM sensor is known to be almost fully catalytic, stainless steel is only partly catalytic. The heat flux reduction of about 30% fully agrees to the measurements in the IPM plasmatron facility in the frame of SACOMAR task 5.4.

In addition to the heat flux measurements several spectroscopic measurement techniques were applied for free stream characteri¬sation. NO molecules were observed by laser induced fluorescence (LIF), while CO was probed by diode laser absorption spectroscopy (DLAS).

From NO-LIF measurements spatially resolved temperature profiles were obtained in the free stream and in front of the flat-faced cylinder models. The absolute temperature level in the free stream was found higher for the low enthalpy test condition FC-2 compared to high enthalpy condition FC-1. This result can only be explained by differences in the chemical gas composition inside the facility's reservoir which shows a higher frac¬tion of CO_2 for FC-2. Since the reservoir condition can be determined from accurate measurements of gas mass flow rate and reservoir pressure, the L2K nozzle flow is an excellent test case for validation of thermochemical models of Martian atmosphere.

Measurements with NO-LIF in the shock layer at different distances to the model surface provided an almost constant temperature level along the stagnation point stream line until the edge of the boundary layer. In addition, the good spatial resolution allowed to extract the position of the bow shock from the lateral profiles and to estimate the shock shape and the shock's stand-off distance. The stand-off distance was found to be 21 mm for the 100 mm model, while it was only about 11 mm for the 50 mm model.

Microwave interferometry and DLAS were mainly applied for velocity measurements. Velocities in the range of 2700 m/s and 3100 m/s were measured for test conditions FC-1 and FC-2, resp. In addition to microwave interferometry, which was only applied at a position 350 mm to the nozzle exit, DLAS measurements was also applied at a more upstream location. As could be expected, only a minor influence was observed in the measured velocities. The measured temperatures, however, show a proper tendency, because significantly higher temperatures are measured at the upstream location. With respect to temperature measurements, it has, however, to be taken into account that DLAS is a line-of-sight method. This property can explain the difference to the measurements with NO-LIF which is a local measurement and provided slightly lower temperatures.

1.3   Specific highlights

Not applicable

1.4   Forms of integration within the work package and with other WPs

The experimental work described in this report has been performed according to the test plan that was defined in task 5.1 of WP 5. The test plan itself is bases on the general requirements which were evaluated in task 4.1 of WP 4. The measured data and further results that were evaluated from measurements will be used as input data for the numerical rebuilding of the tests to be performed by CIRA in task 7.8 of WP 7. In addition the results from the heat flux measurement will be compared to correlated measurements performed in the parallel tasks 5.2, 5.3, 5.4 and 5.5 during the synthesis of the results in task 4.2 of WP 4.

1.5   Problem areas

Not applicable

2   Introduction

A fundamental prerequisite for reliable application of CFD simulation to hypersonic planetary entry flows is a realistic thermochemical model of the planet's atmosphere. Although computational power has grown by orders of magnitudes within the last years, a CFD simulation code that is applicable to 3D configurations is still far away from being able to account for all microscopic effects that have influence on the macroscopic behaviour of a gas at high temperatures. The transfer from microscopic to macroscopic scale is performed by thermochemical modelling. Therefore, in advance to a CFD validation a reliable validation of the implemented thermochemical model has to be performed.

With regard to Earth atmosphere there is a huge experience accumulated and there has been a large number of space missions as well as flight and ground experiments that can be used for model validation. Compared to Earth atmosphere the thermochemical modelling of Martian atmosphere is more complex and covers a wider range of thermodynamical states due to several aspects:

The main objectives of the SACOMAR study are the improvement of experimental and numerical tools to study the aerothermodynamic problems of Martian entry, the achievement of a better understanding of physical phenomena and the creation of a data base. The main objective of the experimental activities in SACOMAR is to provide reliable measured reference data for the validation of thermochemical models of Martian atmosphere and their application within numerical simulation tools. Herein, the principal focus is set to a better understanding of thermochemical relaxation phenomena and its influence on surface heating. Test conditions, model geometries and measurement techniques had been specified in the SACOMAR test plan [1] based on the operational regimes of the individual test facilities and the necessities of future missions to Mars which are exemplarily deduced from the EXOMARS mission.

One of the high enthalpy facilities is the arc-heated facility L2K. In this document the test campaign performed in L2K is described in detail. In particular, it includes a description of the experimental setup, the applied measurement techniques, test procedures and all results obtained from the measurements.

3   Experimental Setup

3.1   L2K Facility

L2K is one of the two test legs of DLR's arc heated facilities LBK which have been playing an important role in the qualification and testing of TPS components and materials in the frames of several European and German programmes, as e.g. Hermes, MSTP, ALSCAP, X-38, ASTRA, etc. Additional activities like tests on the HYFLEX tile model, the ablator material of the USERS capsule, some preparatory activities for the MARS PREMIER programme, etc. allowed the LBK team to gain more experience in aerothermodynamics and qualification of TPS-components for different planetary entry conditions.

A sketch of LBK is shown in Fig. 1. The L2K test leg is equipped with a Huels type arc heater with a maximum electrical power of 1.4 MW that is used to transfer the working gas to a high enthalpy state. At its downstream end the arc heater is connected to a convergent-divergent nozzle which accelerates the gas to hypersonic velocities. After passing the nozzle exit the accelerated gas enters the test chamber where it forms a free jet. Depending on the nozzle setup Mach numbers between 4 and 8 at Reynolds numbers up to 10000/m can be achieved. Models can be exposed to cold wall heat flux rates up to 4 MW/m^2 at stagnation pressures up to 250 hPa. A more detailed description of the facility can be found in [2,3].

One of the main advantages of the L2K arc heater is its flexibility, since it can easily be operated with various gases or gas mixtures. In addition to air, argon, nitrogen and carbon dioxide have intensively been used during the recent years [4,5]. Components for storage and supply of those gases are permanently available. As specified in the test plan [1] L2K was operated with a gaseous mixture consisting of 97% carbon dioxide and 3% nitrogen during the SACOMAR test campaign.

Fig. 1: Sketch of the LBK facility

The huge test chamber of L2K is equipped with several windows allowing for the application of non-intrusive diagnostic tools, in particular optical diagnostic techniques for the characterisation of high enthalpy flow fields [6,7,8]. Emission spectroscopy, absorption spectroscopy, diode laser spectroscopy and laser induced fluorescence spectroscopy on NO and two-photon laser induced

fluorescence on oxygen atoms can be applied providing valuable information on the flow properties. Rotational and vibrational temperatures, densities, flow velocities, and shock stand-off distances can be measured. The techniques are permanently available and continuously used at LBK. Complementary to the spectroscopic tools intrusive techniques are applied to measure cold wall heat flux rates and Pitot pressure profiles [9,10].

3.2   Model geometries

Two model geometries were specified in the test plan [1] for the test campaign in L2K. Both geometries are flat-faced cylinders with rounded edges, but different diameters. A principal sketch is given in Fig. 2: Model geometry.Fig. 2. The first geometry is the so-called "standard ESA geometry" with a diameter of 50 mm and an edge radius of 11.5 mm. This geometry had been established as a standard for material characterization about 25 years ago. The second model has a larger diameter of 100 mm, but an identical edge radius of 11.5 mm.
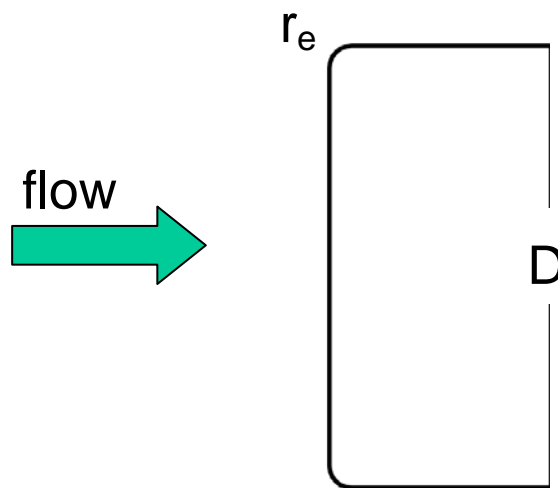

Fig. 2: Model geometry.

Several models with the specified geometries were manufactured in order to apply different measurement techniques. For measurements that cannot be completed within a few seconds, e.g. the laser induced fluorescence technique, the water-cooled models shown in Fig. 3 were prepared. Since the model is permanently exposed to the high enthalpy flow during the measurements, cooling is required to protect the models from overheating.

For short-term measurements non-cooled models were prepared. For cold wall heat flux measurements with the HFM sensor the models shown in Fig. 4 were used. A special plug in the centre part of the model houses the sensor. The design allows for an exchange of the sensor and for local measurements at the stagnation. Another non-cooled model is shown in Fig. 5. It can be used for cold wall heat flux measurements measurements with a slug calorimeter. Again, a special plug is used to house the calorimeter device.

D = 100 mm   D = 50 mm

Fig. 3: Water-cooled flat-faced cylinder models.

D = 100 mm   D = 50 mm

Fig. 4: Flat-faced cylinder models for measurement with the HFM sensor.

Fig. 5: Flat-faced cylinder model for measurements with a slug calorimeter.

3.3 Measurement techniques

Several measurement techniques were applied in order to

- show compliance to the specified test conditions,
- measure cold wall heat fluxes at the models' stagnation point,
- characterize the properties of the free stream and inside the shock layer.

Standard measurement techniques for Pitot pressure, reservoir pressure and gas mass flow rate are applied to demonstrate compliance to the test conditions. All other measurement techniques will be described in following subsections.

3.3.1 Cold wall heat flux measurements

Different measurement techniques were applied for the evaluation of the cold wall heat fluxes in the stagnation point. For reference measurements a commercial heat flux microsensor (HFM) was applied. A photograph of the sensor itself is shown in Fig. 6. Due to its small dimension HFM can be used for local measurement of the stagnation point heat flux. Its response time is less than 1 milliseconds which allows for short-time measurements using the non-cooled models shown in Fig. 4.
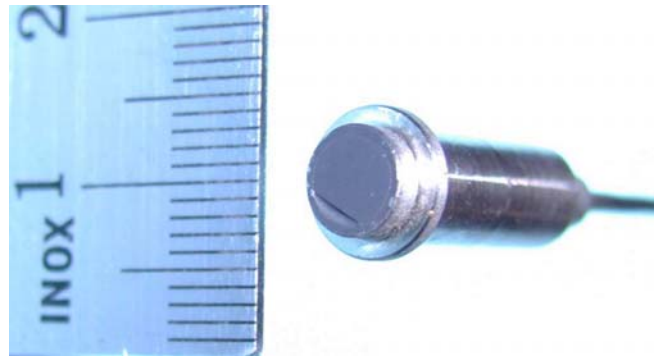

Fig. 6: HFM sensor.

In addition to the HFM sensor a newly designed slug calorimeter was applied. The model assembly is shown in Fig. 5, a sketch of the model's interior parts is given in Fig. 7. The sketch shows that the external shape body of the plug calorimeter is exchangeable. So, a single slug calorimeter can be used for the measurements on the two flat-faced cylinder geometries.
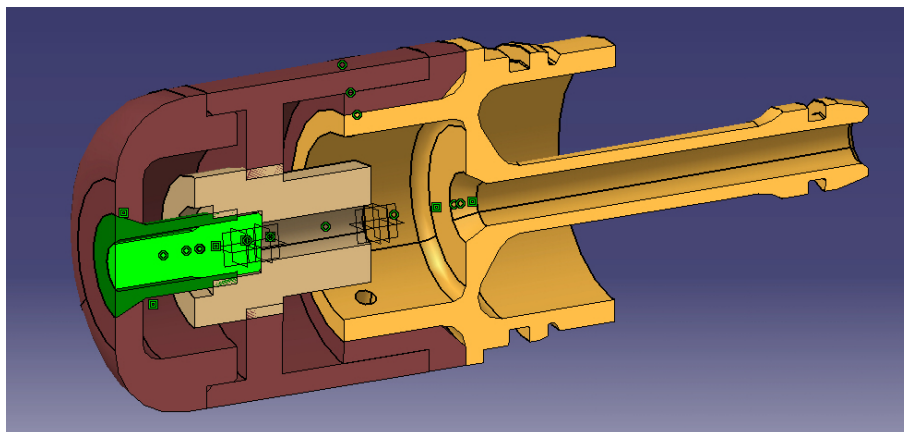

Fig. 7: DLR's slug calorimeter.

The slug calorimeter itself is equipped with two thermocouples which are installed at two different depths on the calorimeter's axis very close to the front surface. From their signals the surface temperature and the surface heat flux are evaluated after test by an inverse thermal analysis. Similar to the HFM sensor, the measurements with the slug calorimeter can be performed within several seconds.

3.3.2   Microwave interferometry

The microwave interferometry is applied at LBK to measure the density of electrons and the free stream flow velocity. By measurement of the phase shift of a microwave beam crossing the free stream perpendicularly the system is able to evaluate the electron density. The main advantage of microwave interferometry is the fact that it is a non-intrusive technique with a high temporal resolution. Therefore, it allows for direct measurement of the electron density, but also velocity measurements can be performed based on temporal fluctuations of the electron density from two individual measurements at different locations.

A sketch of the interferometer is presented in Fig. 8. It consists of two microwave units with antenna, one is emitting a microwave beam at 25.5 GHz and the other acts as a reciever. The microwave emitters and detectors are placed on opposite sides of the free stream inside the test chamber. When the flow is established the presence of free electrons lowers the dielectric permittivity and decreases the phase length of the plasma path. Within the electronic unit, this phase shifted signal is compared to the unaffected signal of the reference path. The measured phase shift is used to derive the line of sight integrated electron density.

A time resolved signal of the electron density can be obtained in density modulated plasmas with the help of an oscilloscope connected to the electronic unit. When using two microwave interferometers and knowing the relative distance of the optical paths, the fast time response of the signal allows to extract information of the velocity. The control unit is able to time correlate the data from the two channels. The velocity is then available as calibrated voltage signal for data acquisition.
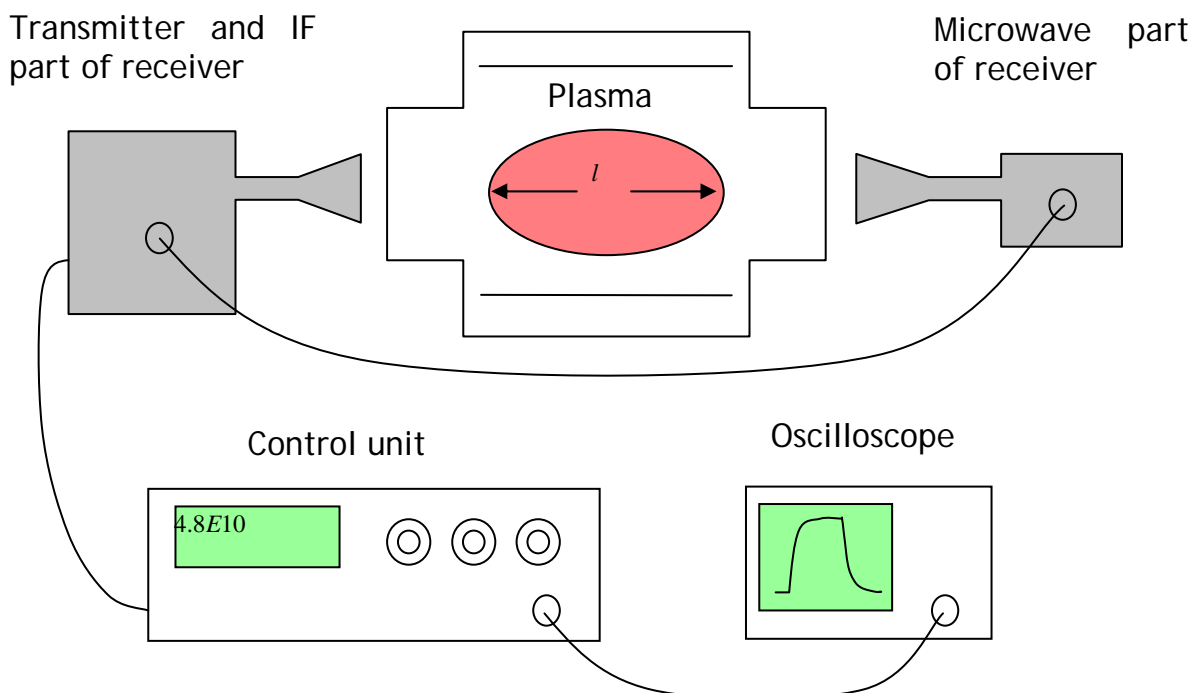

Fig. 8: Microwave interferometry setup for electron density measurements.

A picture of the setup in the L2K facility is shown in Fig. 9. It shows the nozzle exit and the emitters and receivers of the microwave interferometers with a fixed distance between the optical paths of 200 mm.

Fig. 9: Experimental setup for microwave interferometry in L2K.

3.3.3   Laser induced fluorescence spectroscopy

Laser induced fluorescence is characterised by an excellent dynamic range and high detection sensitivity that allow for measurements with a good spatial resolution. The technique is selective for single quantum states (internal energy, electronic, vibrational and rotational). Using appropriate optical setups the technique can be applied to differ¬ent target species like NO, O2, CO, CN, and C2 molecules and N, C and O atoms. An extensive calibration of the technique is required, in par¬ticular at high density conditions when quenching becomes important.

The setup used for LIF measurements in the L2K facility is shown inFig. 10. The main components are a tunable excimer laser (Lambda Physics LPX150), a dye laser system (Scanmate 2E, Lambda Physics), and the detection system. The excimer laser is operated with XeF in the broad-band mode to emit light pulses with a wavelength of 351 nm and a duration of 23 ns, with an energy of 200 mJ per pulse. The light from the excimer laser is used to pump the dye laser.

When using Coumarin 4700 as a dye, the setup is able to probe NO, CO and O atoms. The exci¬tation wavelength for NO (225-226 nm) can be gen¬erated using this dye. Light pulses with an energy of 5-7 mJ per pulse and a linewidth of 0.0015 nm could be generated in the range of 220-240 nm. A UG 5 filter was used for the detection of the NO fluorescence.

LIF measurements on NO molecules were performed by scanning the full tuning range of the laser with wave¬length increments of 0.5 pm at a repetition rate of 3 Hz. Synchroni¬zation of the laser pulse and camera illumination was achieved by a photodiode and was controlled with an oscil-loscope. Illumination time of the CCD-camera is 200 ns. In order to avoid detection of parasitic emission from the model, the laser pulses were synchro¬nized to the illumina¬tion interval.
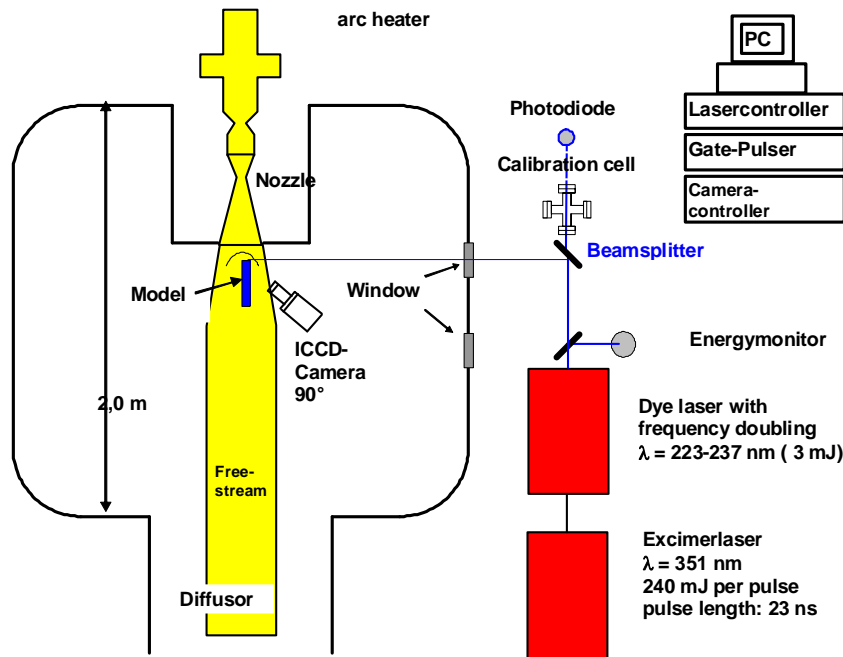
Fig. 10: Experimental setup used for LIF measurements.

3.3.4 Diode laser absorption spectroscopy

Diode laser absorption spectroscopy (DLAS) can be applied for the measurement of several physical properties in a flow field. Recently diode lasers were developed, which emit in the infrared region at room tem¬perature and allow to probe CO with high sensi¬tivity. In general, the principal output is the flow velocity, additionally values of transla¬tional temperature and partial density or partial pressure of the target species can be extracted from the measurements.

DLAS is a line-of-sight-technique which means that data evaluation is based on the assumption of a homogeneous flow field. Nevertheless, it can successfully be applied as long as the deviation from homogeneity are small which has been proven valid for the L2K free stream by Pitot pressure and heat flux measurements.

For the measurements in L2K the DLAS technique was applied on CO molecules. The experimental setup is shown in Fig. 11. The main component is the diode laser Nano¬plus DL 100 DFB. It is controlled by a controller unit from Toptica Photonics. The laser is pumped by electric current and operates at a wavelength of 2333.7 nm. By modulation of the electric current and the tem¬perature of the diode the wave length can be changed between 2329.1 nm and 2335.1 nm.

The R7 line was used for most of the measurements since it provided the highest signal intensity. The laser light is passed from the diode through a quartz win¬dow into the test chamber where a mirror is placed that redirects the light through the hypersonic flow field to a photo detector with a response of 10 MHz from Thorlabs. For exact wavelength determination parts of the incident light is passed through either a Germanium etalon or a reference cell filled with CO.

Assuming homogeneous physical properties in the volume the veloc¬ity is easily extracted from the spectral shift of the absorption frequency:

$$\Delta f = f - f_0 = f_0 \cdot \frac{v \cos \vartheta}{c} \ ,$$

where v is the velocity to be measured, f_0 the absorption frequency of the target particle at rest, c the velocity of light and ϑ the angle between the light path and the flow direc¬tion.
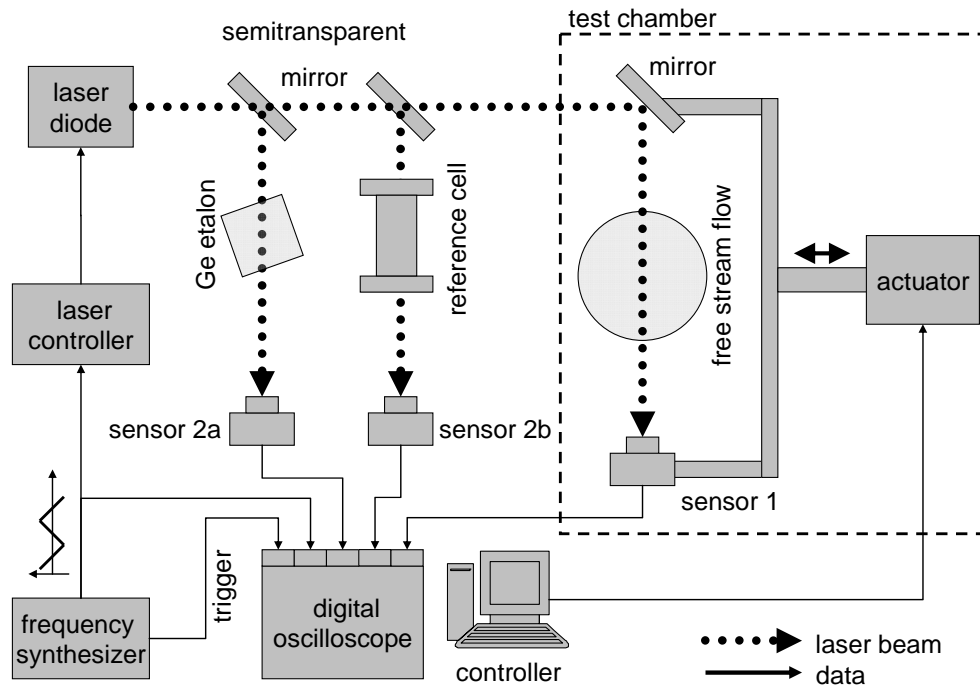
Fig. 11: Setup for diode laser absorption spectroscopy (DLAS).

The translational temperature of a Doppler broadened spectral line can then be deter¬mined from the half width f_d at half height:

$$f_d = \frac{f_0}{c} \cdot \sqrt{\frac{8kT \ln 2}{m}} \quad .$$

Here k is the Boltzmann constant, m the molecular mass. Finally, the density is deter¬mined using Lambert Beer's absorptions formula:

$$I(f) = I_0(f) \cdot \exp(-k \cdot N \cdot L)$$

with k being the extinction coefficient, N the number density and L the optical path length.

4   Test Conditions

The test conditions for the L2K test campaign were specified in the test plan [1] in terms of total enthalpy and Pitot pressure. The corresponding test matrix for the L2K tests is listed in Table 1. It includes tests with the two model geometries at two enthalpy levels of 13.8 MJ/kg and 9.0 MJ/kg and several Pitot pressures. All tests should be performed in a representative Martian atmosphere consisting of 97% carbon dioxide and 3% nitrogen.

Table 1: Test matrix

Test condition	enthalpy	Pitot pressure	model diameter
	[MJ/kg]	[hPa]	[mm]
FC-1	13.8	80,20	50,100
FC-2	9.0	80,20	50,100

Since total enthalpy values cannot be set directly in L2K, appropriate operating conditions had to be identified in a first step. Several operating conditions were checked by setting the gas mass flow rate and measuring both, mass flow rate and the resulting reservoir pressure. Finally, appropriate operating conditions were found. The corresponding parameters are listed in Table 2. The values indicate that for both test conditions a total enthalpy close to the specified value could be achieved.

Table 2: Operating conditions

Test condition	Gas mass flow rate	Reservoir pressure	Reservoir temperature	Total enthalpy
	[g/s]	[hPa]	[K]	[mm]
FC-1	41.2	1080	3820	13.5
FC-2	41.2	920	3260	9.1

In a second step compliance to the specified pressure levels was demonstrated by Pitot pressure measurements at several locations in the free stream. For test condition FC-1 the results of the measurements are shown in Fig. 12. At a distance of 90 mm to the nozzle exit a Pitot pressure of 80 hPa could be achieved on the axis of the flow field, while a Pitot pressure of 20 hPa was found further downstream at a distance of 380 mm. After checking the Pitot pressure on the axis radial pressure profiles were measured. The profiles demonstrate radial homogeneity of the flow at these two locations.

For test condition FC-2 the corresponding measurements are plotted in Fig. 13. At this condition a pressure of 20 hPa was obtained at a distance of 350 mm. At a distance of 90 mm to the nozzle exit which is the minimal distance for model measurements a Pitot pressure of 75 hPa was obtained which is slightly below the specification of 80 hPa. The profiles demonstrate flow homogeneity in radial direction for test condition FC-2 as well. Flow homogeneity is also supported by the visual impression from the flow field shown in Fig. 14.
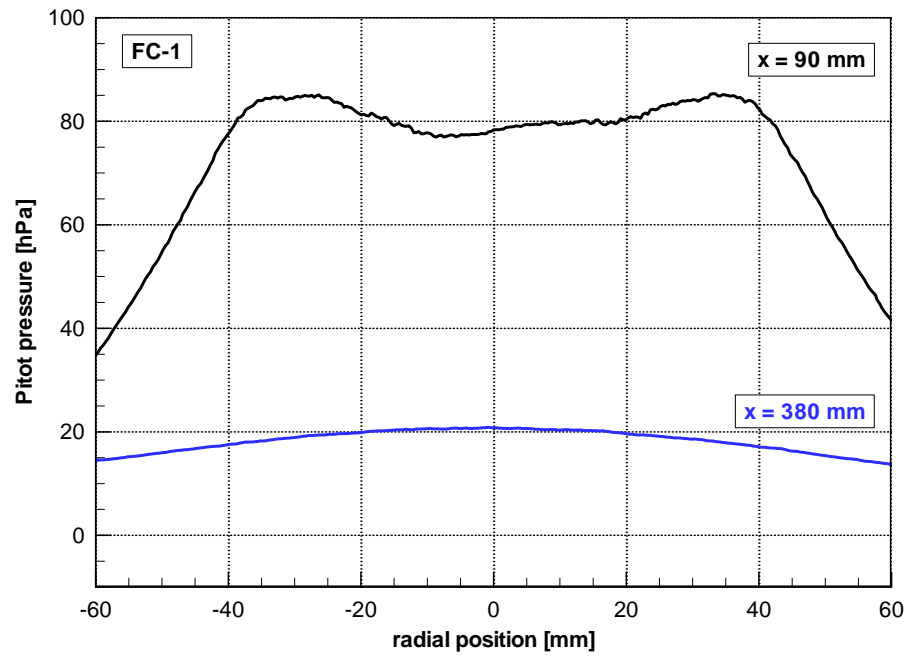
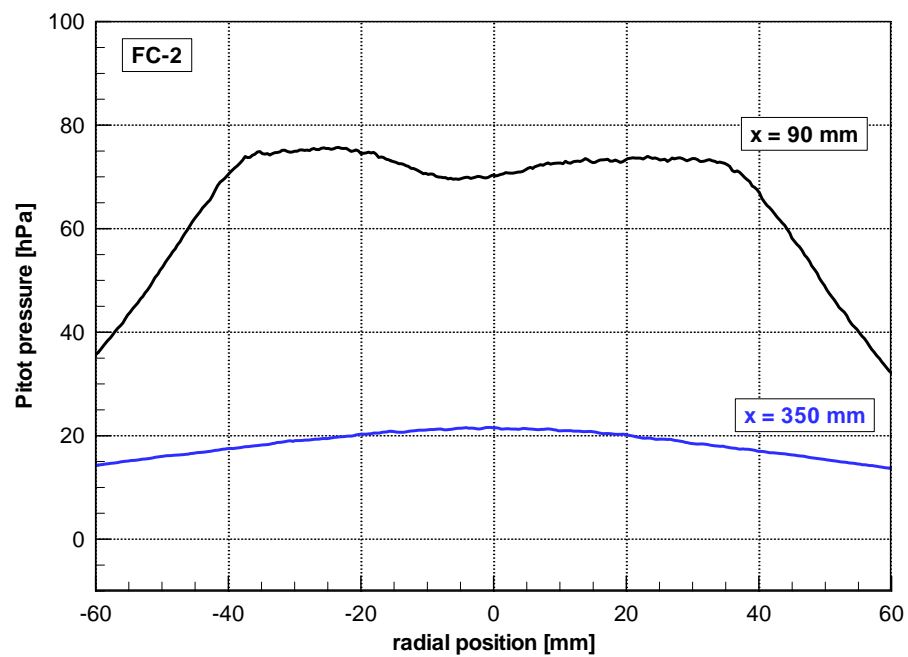**Fig. 12: Radial Pitot pressure profiles at test condition FC-1.**

Fig. 13: Radial Pitot pressure profiles at test condition FC-2.
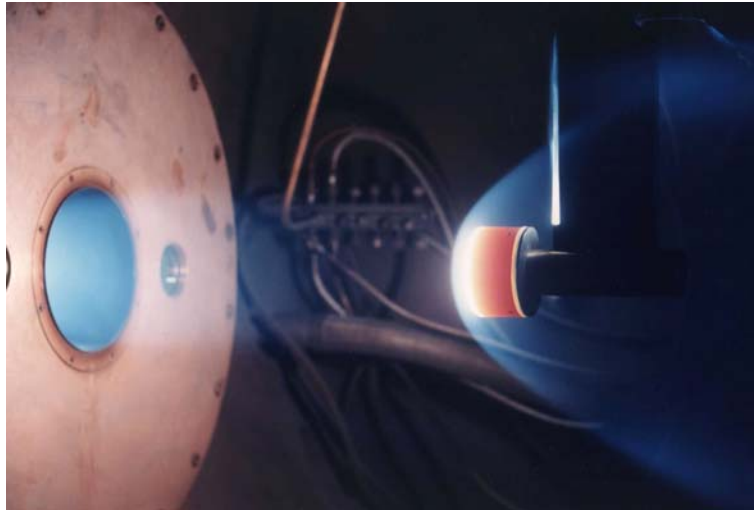
Fig. 14: Flat-faced cylinder model in hypersonic flow.

5   Experimental Results

The main objective of the experimental activities in SACOMAR is to provide reliable measured reference data for the validation of thermochemical models of Martian atmosphere and their application within numerical simulation tools. Principal focus is set to a better understanding of thermochemical relaxation phenomena and its influence on surface heating.

To meet this objective heat flux measurements were performed using several measurement techniques. Additionally, different optical and spectroscopic techniques were applied to characterize the free stream in order to provide realistic input data for the numerical rebuilding of the tests in WP 7.
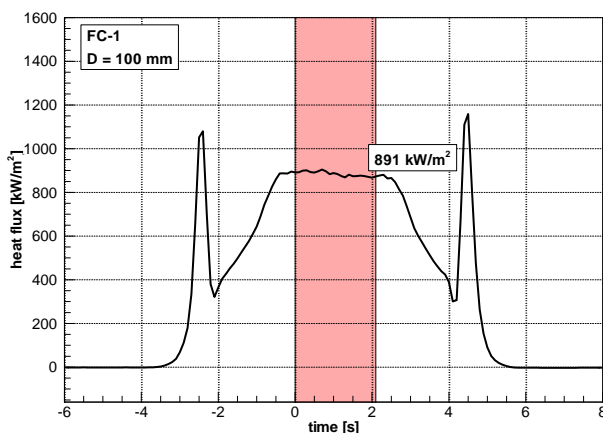
5.1   Heat Flux measurements

Two different measurement techniques were applied for the evaluation of the cold wall heat fluxes in the stagnation point, i.e.

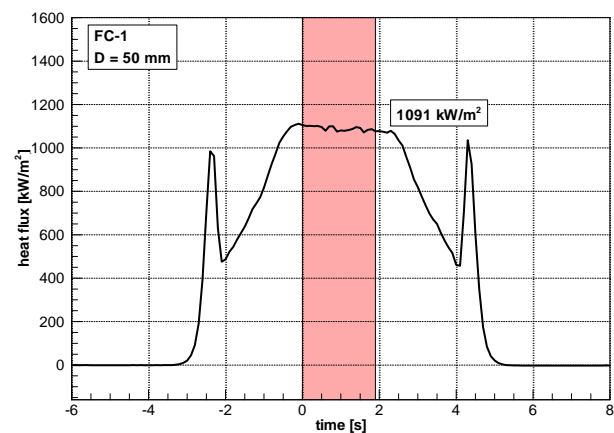- a commercial heat flux microsensor (HFM),
- a slug calorimeter.

5.1.1   HFM sensor

The HFM sensor is a commercial sensor that provides a signal which is proportional to the heat flux. Due to its small dimension HFM can be used for local measurement of the stagnation point heat flux. Its response time is less than 1 milliseconds which allows for short-time measurements using non-cooled models.

The plots in Fig. 15 very clearly demonstrate the fast response time of the HFM sensor. The curves show the time history of the stagnation point heat flux during the measurements at test condition FC-1 on the 50 mm and 100 mm model, resp. For the measurement the model was moved from the background of the test chamber to the axis of the flow field. Here it remained for about 2 seconds before it was removed out of the flow field again. On its way into and out of the flow field the models has to pass the boundary of the free stream at a distance of about 150 mm to the axis of the flow field. Although the time of the passage is rather short the sensor is able to resolve the correlated peak in heat flux.

p = 20 hPa, D = 100 mm   p = 20 hPa, D = 50 mm

Fig. 15: HFM measurements at test condition FC-1.

Relevant heat flux data are obtained only during the time period when the sensor is placed on the axis. Therefore, this period is marked by a red background colour in the plots. For the measurements at FC-1 a nearly constant signal was obtained. Since the stand-off distance of the bow shock is smaller for the 50 mm model, the stagnation point heat flux is higher compared to the 100 mm model.

The measurements at test condition FC-2 are plotted in Fig. 16. Due to the lower level of total enthalpy the measured heat fluxes are below the values for FC-1. Again, a nearly constant heat flux signal was obtained and a significantly higher heat flux was measured for the 50 mm model. All measurements with the HFM sensor are summarized in Table 3.
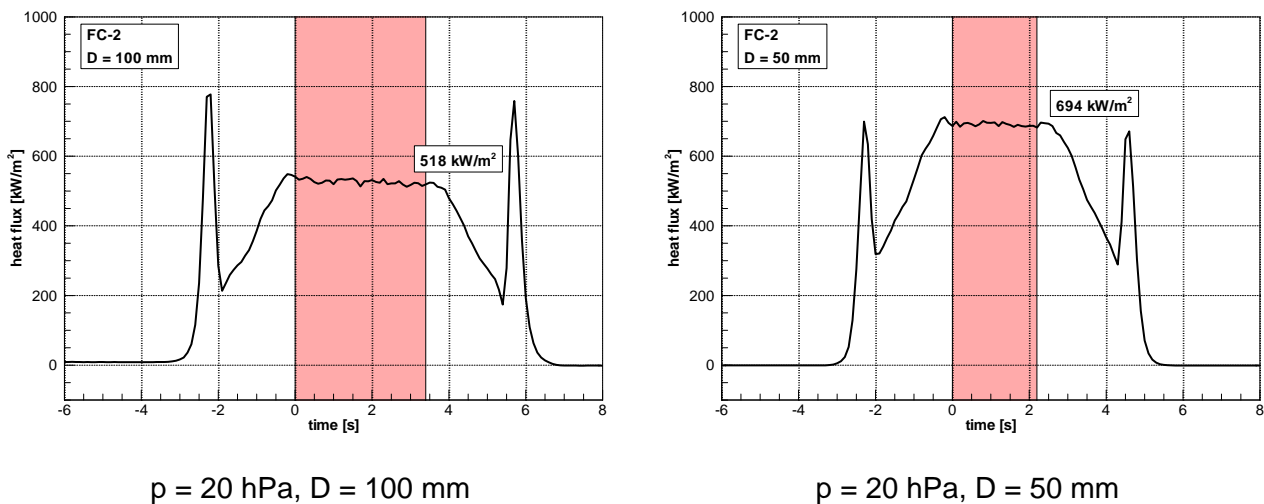

p = 20 hPa, D = 100 mm   p = 20 hPa, D = 50 mm

Fig. 16: HFM measurement at test condition FC-2.

Table 3: Heat fluxes measured with the HFM sensor

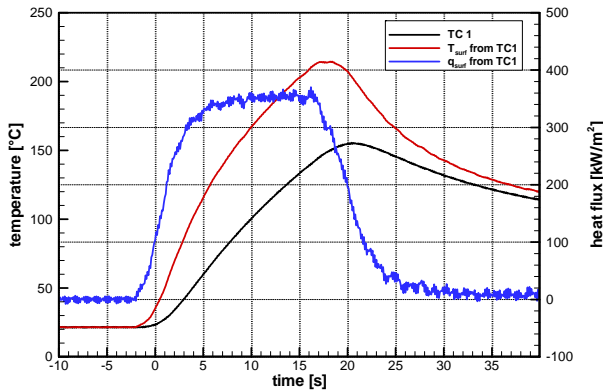| Test condition	Model diameter	Pitot pressure	Heat flux rate
	[mm]	[hPa]	[kW/m^2]
FC-1	100	20	891
	50	20	1091
FC-2	100	20	518
	50	20	694

5.1.2 Slug calorimeter

Setup and working principle of the slug calorimeter were already described in section 3.3.1. For the measurements in L2K a slug made of stainless steel was used. The slug was equipped with two type-K thermocouples installed at a distance of 2 mm and 3 mm from the front surface.

The evaluation of the heat flux at the front surface is based on the thermocouple measurements. From the measured temperature history the correlated time histories of surface temperature and surface heat flux are reconstructed using an inverse technique [11] based on the sequential function specification method [12].
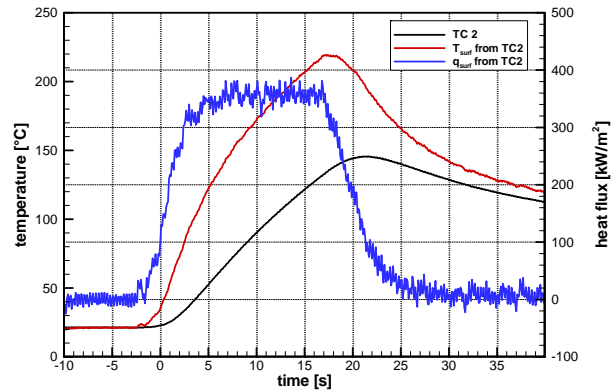
Principally, only one thermocouple measurement is required for heat flux evaluation. The use of two thermocouples provides an intrinsic consistency check for data evaluation, since both measurements can be used separately for heat flux determination and consistency is proved by agreement of the two results. This strategy is demonstrated based on the plots in Fig. 17 which

shows the results of data evaluation for the measurement on the 100 mm model at test condition FC-2 and 20 hPa. The test procedure of this test was similar to the HFM measurements. First the model was moved from the background of the test chamber to the center of the flowfield where it arrived at t = 0 and remained for 15 seconds. Afterwards the model was moved out the flow again. The black line in Fig. 1Fig. 17a shows the temperature history measured by thermocouple TC 1 in a depth of 2 mm. The correlated surface temperature is given by the red line which clearly shows that the model gets heated already on its way to the final test location. As it had been indicated by the HFM measurement this phenomenon is mainly related to the passage of the freestream boundary. After arrival at the final position both, the temperature of TC1 as well as the surface temperature increase continuously. The blue line indicates that this increase corresponds to a constant surface heat flux of 355 kW/m^2.

There are no major differences between the data evaluations based on the measurement of thermocouple TC1 and TC2. The noise level on the reconstructed surface data, however, is larger for the TC2 measurement. As comes out from Fig. 18 this phenomenon was observed for the measurement at test condition FC-1 and all other measurements with the slug calorimeter. It can be explained by the larger installation depth of thermocouple TC 2 which is responsible for a larger amplification of signal noise when applying the inverse method.
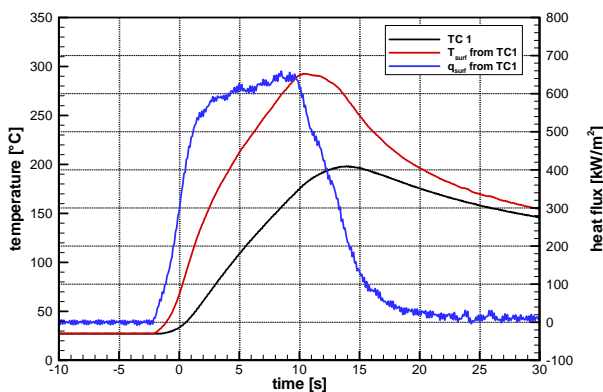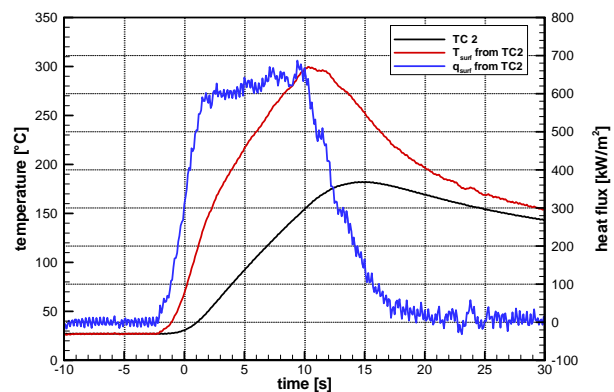

(a) based on TC1 measurement (b) based on TC2 measurement

Fig. 17: Slug calorimeter measurement at test condition FC-2 (p = 20 hPa, D = 100 mm).

(a) based on TC1 measurement (b) based on TC2 measurement

Fig. 18: Slug calorimeter measurement at test condition FC-1 (p = 20 hPa, D = 100 mm).

All heat fluxes determined from measurements with the slug calorimeter are listed in Table 4. At both test conditions the data show that higher stagnation point heat fluxes are obtained for the

50 mm model compared to the 100 mm model. Furthermore, the heat flux considerably increase when the Pitot pressure is increased from 20 hPa to 80 hPa.

Table 4: Heat fluxes measured with the slug calorimeter

Test condition	Model diameter	Pitot pressure	Heat flux rate
	[mm]	[hPa]	[kW/m^2]
FC-1	100	20	640
	50	20	740
	50	80	1380
FC-2	100	20	355
	50	20	440
	50	80	630

5.2   Microwave Interferometry

When operating the L2K facility at the two test conditions FC-1 and FC-2 the electron density was found below the detection limit of the microwave interferometer, i.e. lower $5 \cdot 10^8$/cm^3. Because of the permanent drift of the signal's baseline lower quantitative values could not be determined. The temporal fluctuations from the two detectors, however, could still be evaluated and velocity data could be obtained. At a distance of 350 mm to the nozzle exit a velocity of 3100 m/s was determined for test condition FC-1, while for FC-2 a value of 2700 m/s was measured.

Table 5: Velocities measured by microwave interferometry

Test condition	Velocity
	[m/s]
FC-1	3100
FC-2	2700

5.3   Laser Induced Fluorescence

Laser induced fluorescence was applied on NO molecules to determine radial temperature profile in the free stream as well as in the shock layer in front of the flat-faced cylinder models. Fig. 19 shows a spectrum that was measured in the L2K free stream at flow condi¬tion FC-2. The measurement was taken at a distance of 350 mm to the nozzle exit plane. For data reduction purposes the measured spectrum is compared to analytical spectra first. A best least square fit is then obtained by varying temperature, laser line width, saturation parameter, and wavelength offset. The procedure and relations are described in more detail in [13]. For the measured spectrum shown in Fig. 19 the best fit is plotted in Fig. 20. For this particular spot a temperature of 488 K is obtained.

Performing identical procedures for each measurement spot along the part of the laser light path that is visible to the detector the rotational temperature profile shown in Fig. 21 is obtained. The detector could resolve a line of approximately 200 mm in total. A nearly constant temperature of 472 K is measured in the core of the flow field. Towards the free stream boundary at the left hand side of the plot the temperature decreases almost linearly to a value of 330 K.
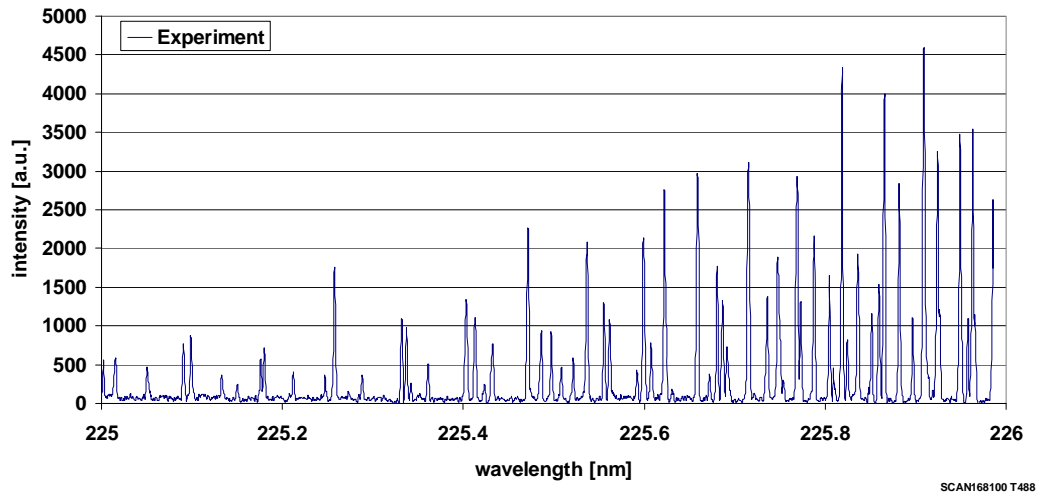
SCAN168100 T488

Fig. 19: NO fluorescence spectrum measured at test condition FC-2.
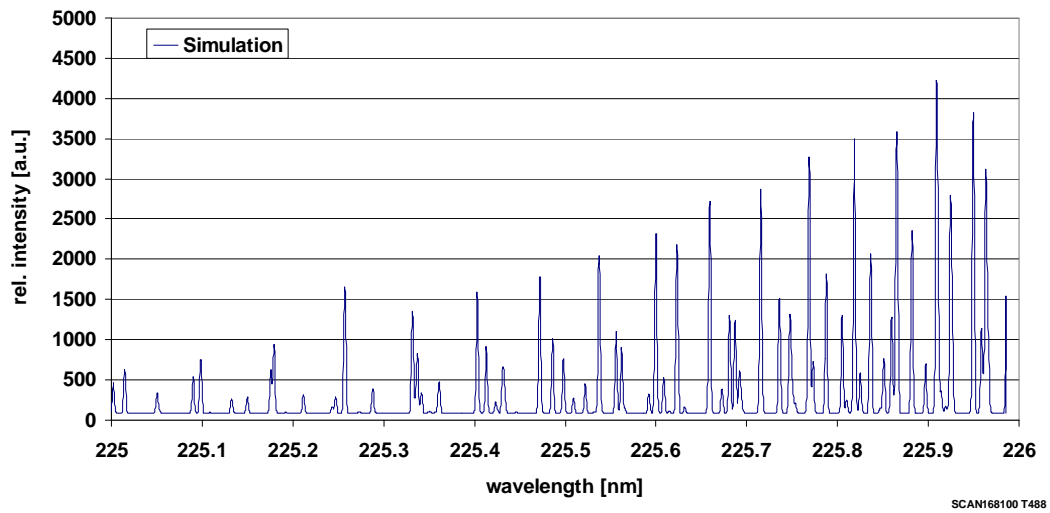

SCAN168100 T488

Fig. 20: Analytical best fit to the spectrum in Fig. 19.

Using the temperature data the NO partial density in the free stream can be deduced by comparing the measured intensities to intensities from calibration spectra, which were taken at room temperature and known NO concentration. From comparison a partial NO density of $2.4 \cdot 10^{-6}$ kg/m^3 is obtained at model location for test condition FC-2.
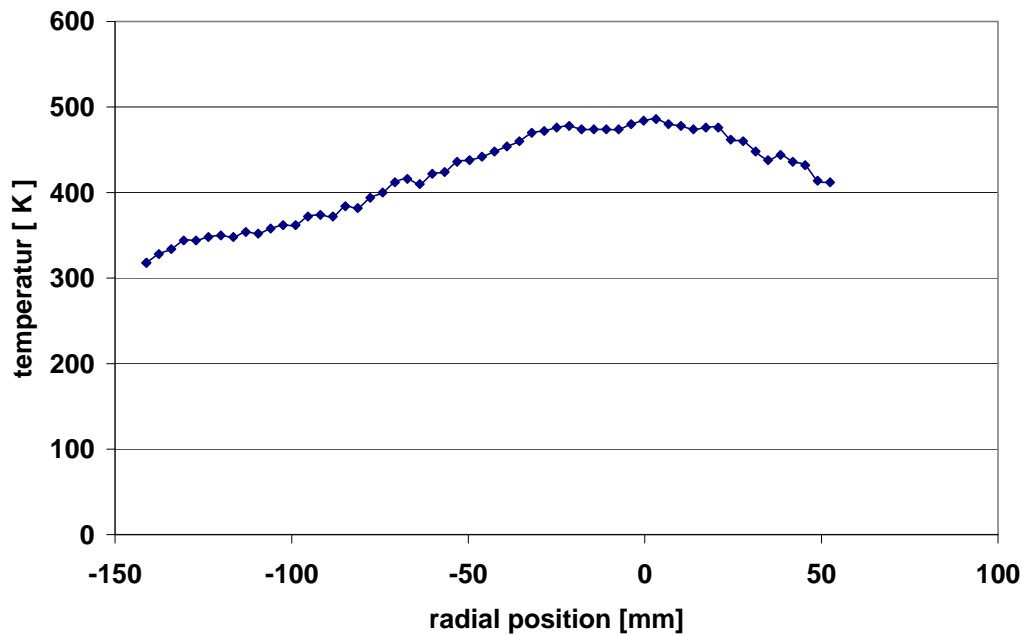
Fig. 21: Temperature profile for test condition FC-2 (distance to nozzle exit d = 350 mm).

In Fig. 22 the temperature profile obtained at test condition FC-2 is compared to the analogous measurement at test condition FC-1. The FC-1 profile is analogous to the temperature profile for FC-2, but the absolute temperature values are about 80° lower with a maximum value of 420 K in the center, although the total enthalpy level is lower for FC-2.
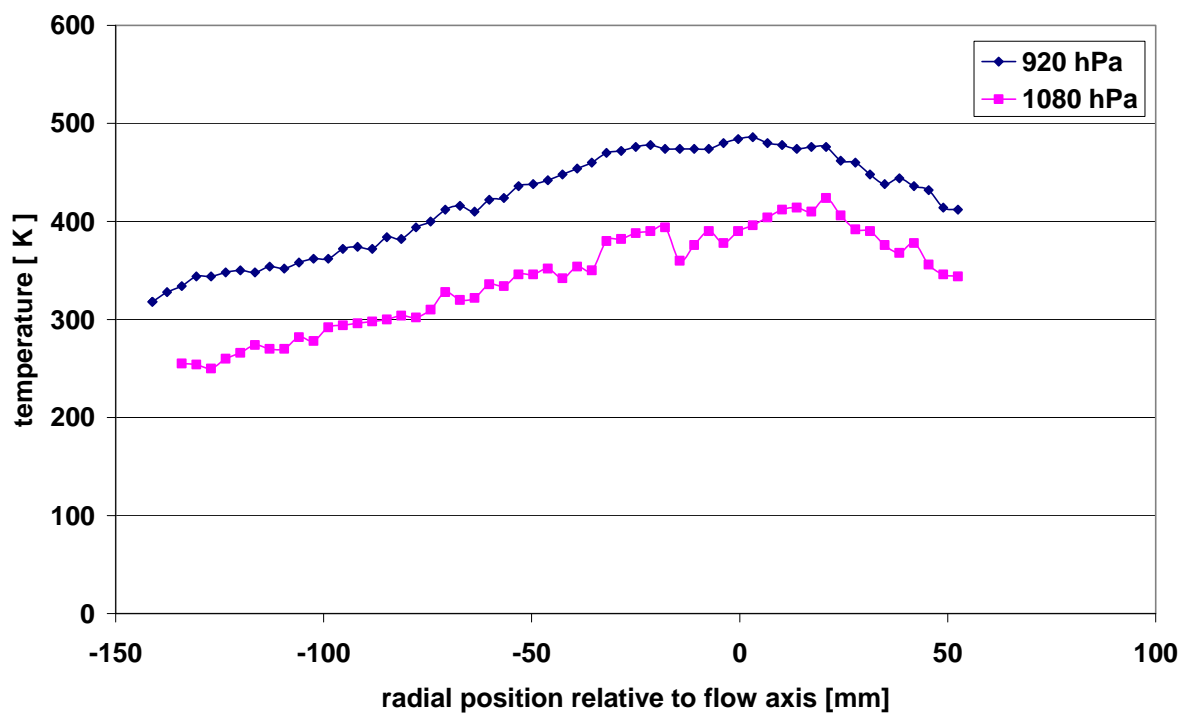

Fig. 22: Comparison of temperature profiles at a distance of 350 mm.

LIF measurements on NO molecules were also taken in the shock region of the two models. For both models, lateral temperature profiles were taken at various distances to the model surface.

For flow condition FC-2, a temperature profile was measured at a distance of 4 mm to the surface. The results are plotted in Fig. 23. Close to the surface, at 4 mm distance, the shock region is wide, slightly wider than the model diameter of 100 mm. To the sides the temperature is on the free stream level of about 300 K. Within the shock region the measurement shows a fairly constant temperature on a level of 2800 K. Data scattering is increased compared to the free stream measurements, since due to the elevated temperature level different spectral lines overlap which increases the uncer¬tainty of measurements to 8%.
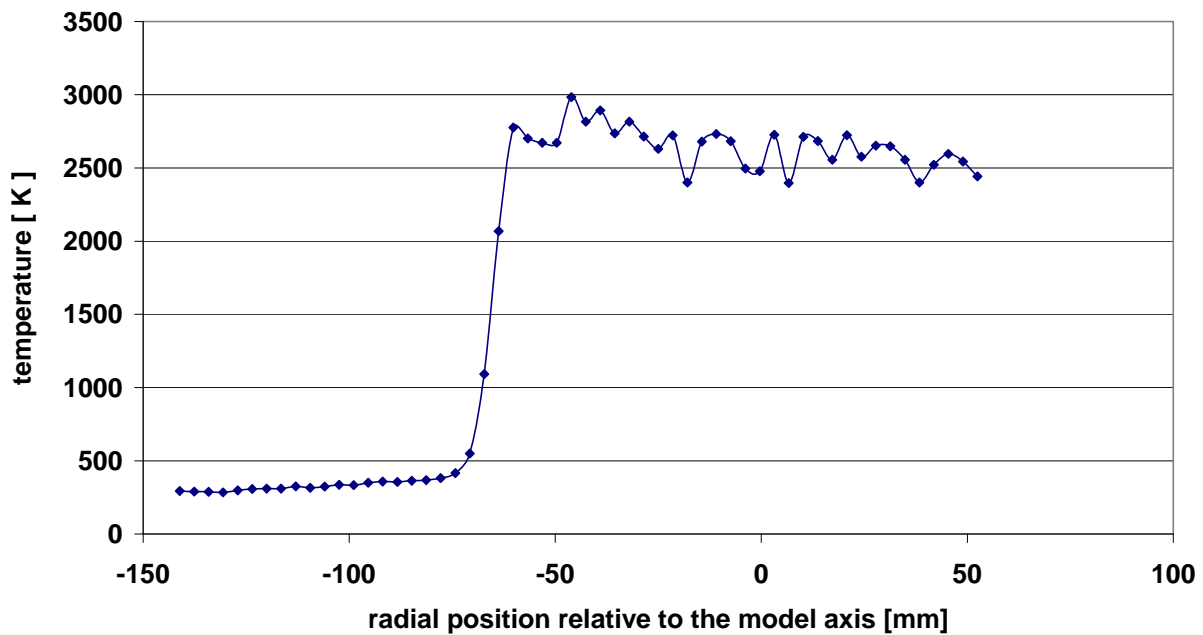

Fig. 23: Temperature profiles 4 mm in front of the 100 mm model at test condition FC-2.

At test condition FC-1, the temperature inside the shock layer is quite homogeneous as well. Due to the higher total enthalpy the temperature level is higher, Fig. 24 indicates an average value of 3760 K at a distance of 3 mm to the model surface.

A special experimental technique was applied for the determination of the shock stand-off distance. At different distances the intensity of a single spectral line at 225.0505 nm was examined. The in-tensity of the spectral line is known to increase with gas temperature. Therefore this simplified technique can be applied to determine the lateral extension of the shock layer. At a dis¬tance of 11 mm the lateral extension of the shock layer is still slightly larger than the model's diameter. At 20 mm, there is only a very narrow area with a high signal inten¬sity, while at 22 mm distance the signal intensity remains at low level for the complete detection path. Therefore, a shock stand-off distance of 21±1 mm can be extracted from the measurements.

Using the 50 mm model with test condition FC-2, measurements have been performed in the shock region at 6 mm distance. Here, an average temperature of 3250 K was measured (see Fig. 25). As expected this value is below the level that was measured in the shock layer of the larger model at flow condition FC-1.
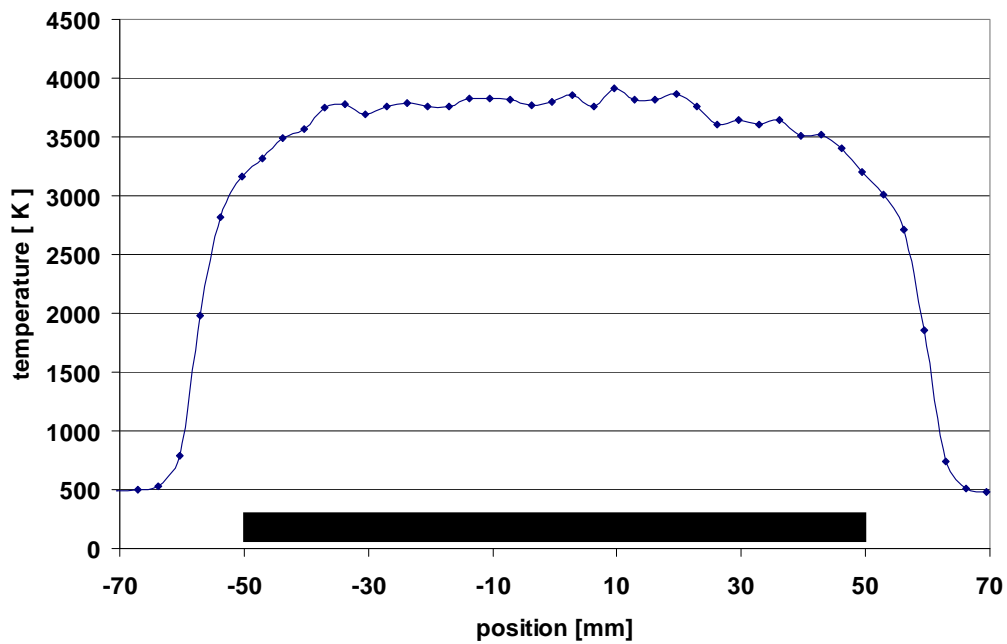
Fig. 24: Temperature profile 3 mm in front of the 100 mm model at test condition FC-1.

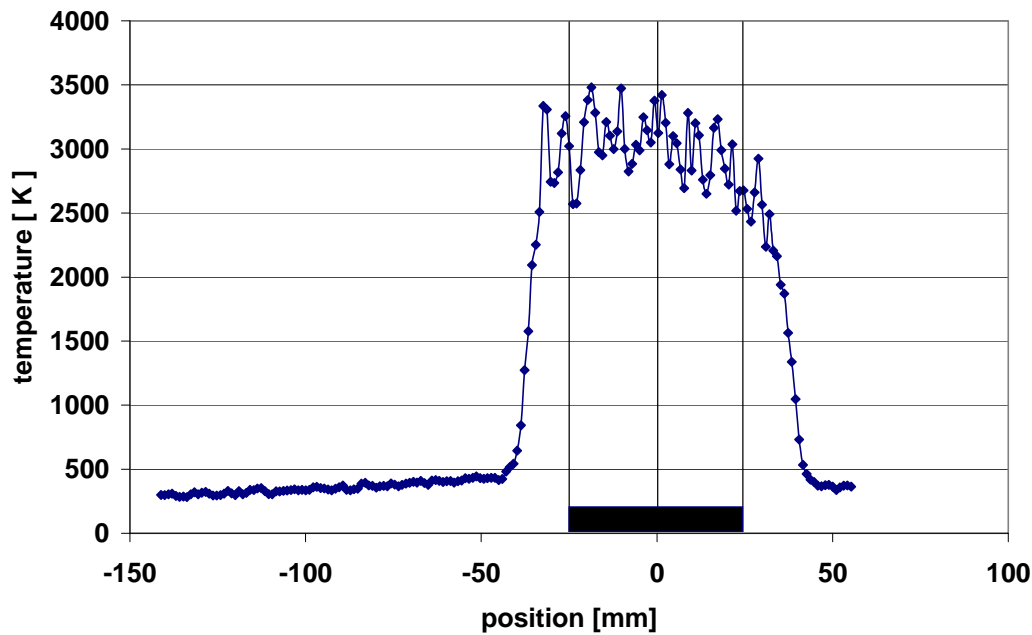**Fig. 25: Temperature profile 6 mm in front of the 50 mm model at test condition FC-2.**

At a distance of 10 mm to the model's surface a homogeneous temperature level can hardly be observed (see Fig. 26). The measurement was taken mainly within the free stream, influenced only close to the axis by the bow shock. Therefore, it can be concluded that the stand-off distance is in the range of 10 mm for this configuration.
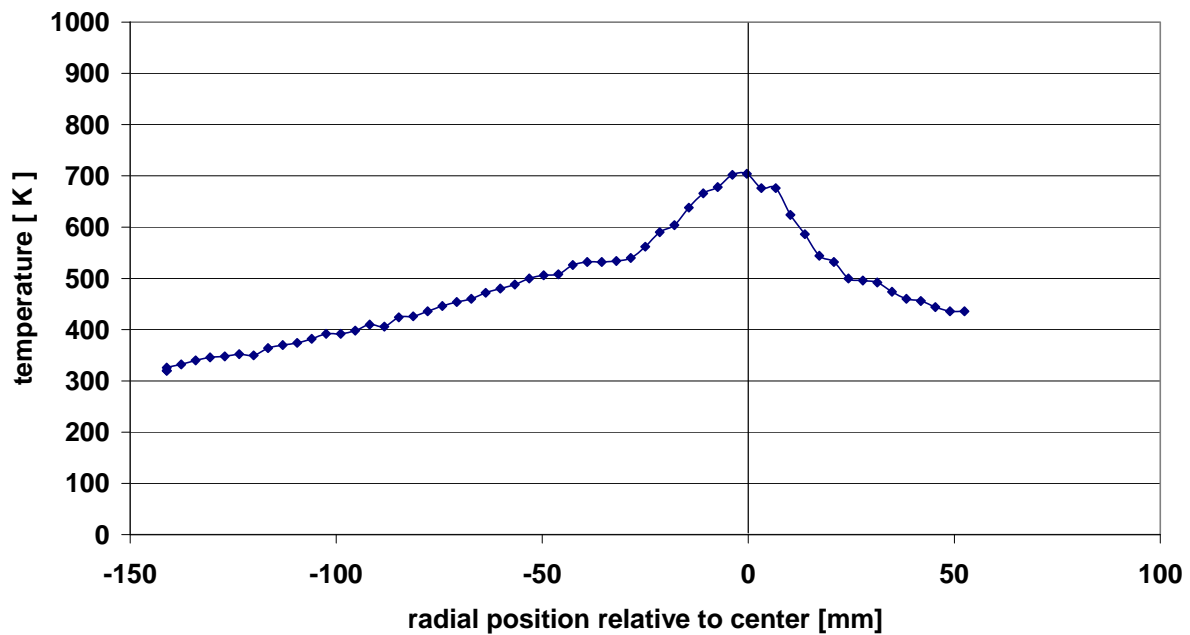
Fig. 26: Temperature profile 10 mm in front of the 50 mm model at test condition FC-2.

5.4   Emission Spectroscopy

In addition to the LIF technique emission spectra were taken from the shock region. This technique did not provide quantitative results, but it clearly identified the main chemical species in the flow field. An Ocean Optics USB 2000 spectrometer equipped with an optical fibre and a collamination lens was used for the measurements. This setup allows to record spectra for the wavelength range from 200 to 850 nm with an spectral resolution of 1.4 nm.

Calibration of the setup was performed by using a tungsten ribbon lamp placed at the position of the measurement volume. Measurements in the free stream region resulted in very low intensity spectra with a fluctuating broad unstructured background. A detailed analysis of these emission spectra is not possible.

In front of the 50 mm model the signal intensities were sufficiently high. A typical spectrum measured for the high enthalpy test condition FC-1 is shown in Fig. 27. As marked in the figure, there are lines from oxygen atoms as well as from CN and C_2 molecules. The strong emission in the short wavelength range at 388 nm, 359 nm and 421 nm and 460 nm are due to the CN violet system, while for longer wavelengths the emission is dominated by the CN red system and the C_2 Swan system. The line emission at 777 nm is related to excited oxygen atoms. The same spectral features appear in the spectra when varying the enthalpy level from test condition FC-1 down to FC-2. Only the intensity of the lines is considerably lower.
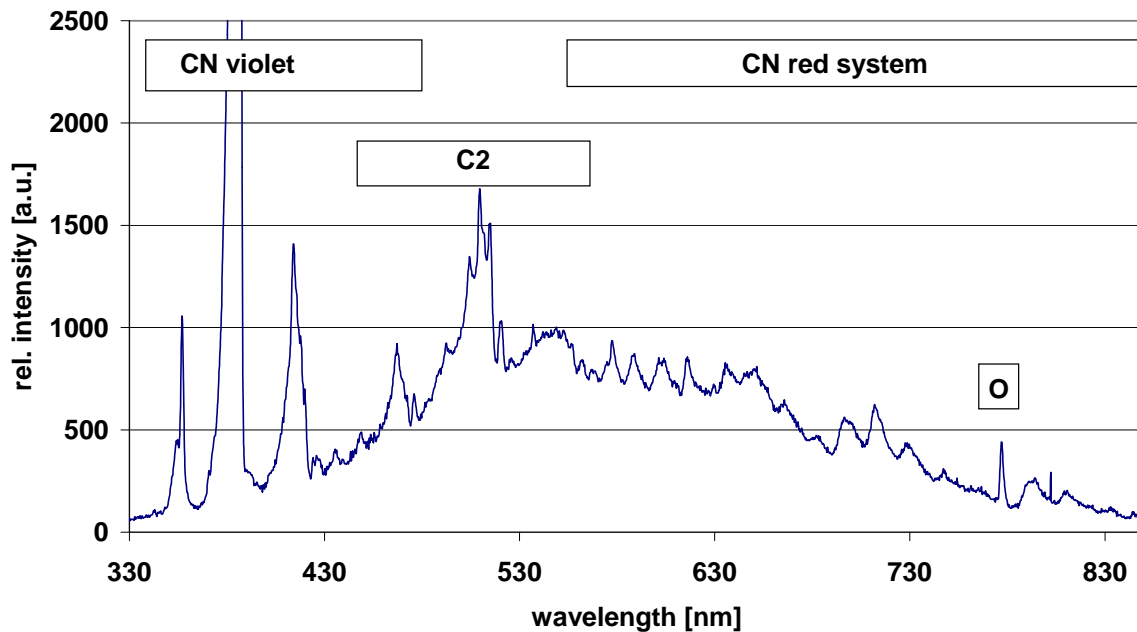
Fig. 27: Emission spectrum taken at test condition FC-1 in front of the 50 mm model.

5.5   Diode Laser Absorption Spectroscopy

The calibration of the DLAS setup for concentration measurements was performed with known amounts of CO filled into the test chamber of the L2K facility at room tempera¬ture. For the measurements the system was setup in a way that the absorption path was inclined by 58° and 63° with respect to the flow axis for distances downstream the nozzle exit plane of 128 mm and 335 mm.

As mentioned earlier, the flow velocity can be extracted from the spectral shift and the gas temperature from the half width of the absorption line, in general (see Fig. 28). For this particular setup more accurate values are obtained if the data are corrected due to the fact that a significant fraction of the absorption path crosses the test chamber's background area where the flow velocity is quite low. The correction is based on a two-layer model with the free stream forming one layer and the background area the other.

For test condition FC-2 and a distance of 335 mm to the nozzle exit the DLAS system provides a constant signal of 2700±110 m/s. For the high enthalpy test condition FC-1 a velocity of 3220±110 m/s was measured. Closer to the nozzle exit, at a distance of 128 mm only slightly lower velocities were measured, namely 2635±80 m/s and 3150±80 m/s.

The corresponding values for the translational temperature of CO at a distance to the nozzle exit of 128 mm are 488 K for FC-1 and 510 K for FC-2. After changing the measurement position to a distance of 355 mm to the nozzle exit the translational temperatures decrease to 360 K for FC-1 and 442 K for FC-2. All DLAS results are summarized in Table 6.

Table 6: Velocities and temperatures measured by DLAS

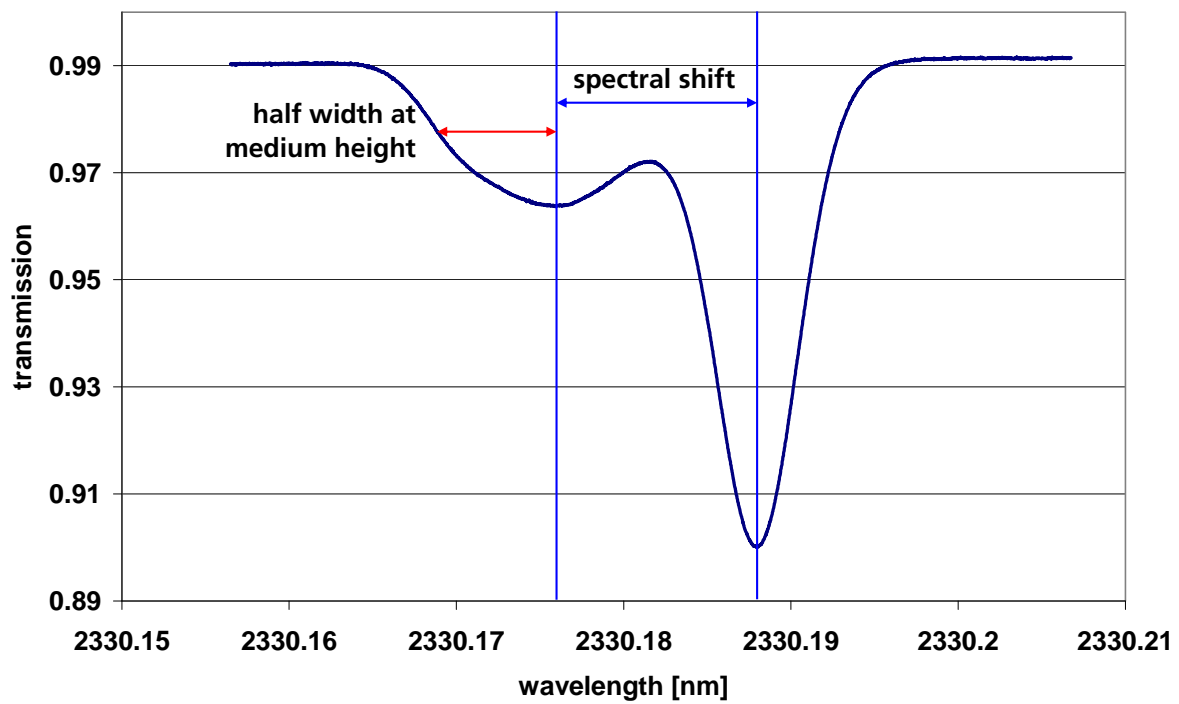| Test condition	Velocity [m/s]		Temperature [K]	
	x = 128 mm	x = 355 mm	x = 128 mm	x = 355 mm
FC-1	3150±110	3220±80	488	360
FC-2	2635±110	2700±80	510	442

Fig. 28: Results from DLAS measurement at flow condition FC-1.

6   Summary and Conclusions

In the frame of the SACOMAR project an experimental test campaign was performed in DLR's arc heated facility L2K. The campaign was run in order to gather experimental data that can be used for the validation of thermo-chemical models that are applied in CFD simulation schemes for Martian entry flow problems. Therefore, all tests were performed at high enthalpy flow conditions in a mixture of 97% carbon dioxide and 3% nitrogen, which represents the chemical composition of the Martian atmosphere.

Two different test conditions had been defined in the SACOMAR test plan. The first test condition FC-1 is characterized by a high total enthalpy of 13.8 MJ/kg. The enthalpy level of the second test condition FC-2 is considerably lower at 9.0 MJ/kg. For these two conditions a large number of measurements was performed both, in the free stream and in the shock layer of two flat-faced cylinder models with diameters of 50 mm and 100 mm.

In a first step, compliance to the specified test condition was demonstrated by Pitot pressure measurements. Additionally, radial homogeneity of the flow field was proved by Pitot pressure profiles.

In the first subset of tests, the cold wall heat flux in the stagnation point of the models was measured with different techniques, i.e. a so-called heat flux microsensor (HFM) and a slug calorimeter made of stainless steel. The results obtained with these techniques are compared in Table 7. The listed values indicate that the slug calorimeter generally provides lower heat fluxes when compared to the HFM measurements. Taking HFM as reference the reduction is between 28% and 36%, i.e. nearly constant. Therefore, the differences might be regarded as systematic. A possible explanation could be the different surface catalycity. The surface of the HFM sensor is known to be almost fully catalytic, while stainless steel is only partly catalytic. The heat flux reduction of about 30% fully agrees to the measurements in the IPM plasmatron facility in the frame of SACOMAR task 5.4.

Table 7: Comparison of heat flux measurements

Test condition	Model diameter	Pitot pressure	Heat flux rate [kW/m^2]	
	[mm]	[hPa]	HFM	Slug calorimeter
FC-1	100	20	891	640
	50	20	1091	740
	50	80	-	1380
FC-2	100	20	518	355
	50	20	694	440
	50	80	-	630

In addition to the heat flux measurements several spectroscopic measurement techniques were applied for free stream characteri¬sation. NO molecules were observed by laser induced fluorescence (LIF), while CO was probed by diode laser absorption spectroscopy (DLAS).

From NO-LIF measurements spatially resolved temperature profiles were obtained in the free stream and in front of the flat-faced cylinder models. The absolute temperature level in the free stream was found higher for the low enthalpy test condition FC-2 compared to high enthalpy condition FC-1. This result can only be explained by differences in the chemical gas composition inside the facility's reservoir which shows a higher frac¬tion of CO_2 for FC-2. Since the reservoir condition can be determined from accurate measurements of gas mass flow rate and reservoir

pressure, the L2K nozzle flow is an excellent test case for validation of thermochemical models of Martian atmosphere.

Measurements with NO-LIF in the shock layer at different distances to the model surface provided an almost constant temperature level along the stagnation point stream line until the edge of the boundary layer. In addition, the good spatial resolution allowed to extract the position of the bow shock from the lateral profiles and to estimate the shock shape and the shock's stand-off distance. The stand-off distance was found to be 21 mm for the 100 mm model, while it was only about 11 mm for the 50 mm model.

Microwave interferometry and DLAS were mainly applied for velocity measurements. Velocities in the range of 2700 m/s and 3100 m/s were measured for test conditions FC-1 and FC-2, resp. In addition to microwave interferometry, which was only applied at a position 350 mm to the nozzle exit, DLAS measurements was also applied at a more upstream location. As could be expected, only a minor influence was observed in the measured velocities. The measured temperatures, however, show a proper tendency, because significantly higher temperatures are measured at the upstream location. With respect to temperature measurements, it has, however, to be taken into account that DLAS is a line-of-sight method. This property can explain the difference to the measurements with NO-LIF which is a local measurement and provided slightly lower temperatures.

7   References

[1]   Esser, B., Gülhan, A., *Test Plan for Experiments*, SACOMAR D 5.1, June 2011.

[2]   Gülhan, A.; Esser, B.; Koch, U.; *Experimental Investigation on Local Aerothermodynamic Problems of Re-entry Vehicles in the Arc Heated Facilities LBK*, AIAA Journal of Spacecraft and Rockets, Volume 38, Number 2, 199-206, 2001.

[3]   Gülhan, A.; Esser, B.; *Arc-Heated Facilities as a Tool to Study Aerothermodynamic Problems of Reentry Vehicles.* in: Lu, F.K.; Marren, D.E. (Eds.): *Advanced Hypersonic Test Facilities*, Progress in Astronautics and Aeronautics, Vol. 198, 375-403, AIAA, 2002.

[4]   Gülhan, A.; Esser, B.; Koch, U; Hannemann, K.; *Mars Entry Simulation in the Arc Heated Facility L2K*, Proc. 4th European Workshop on Hot Structures and Thermal Protection Systems for Space Vehicles, Palermo, Italy, ESA SP-521, 2003.

[5]   Koch, U.; Riehmer, J.; Esser, B.; Gülhan, A.; *Laser Induced Fluorescence and Diode Laser Absorption Spectroscopy Measurements in CO/CO2 Hypersonic Flow of LBK*, Proc. 6th European Symposium on Aerothermodynamics for Space Vehicles, ESA SP-659, Versailles, Frankreich, 2008.

[6]   Koch, U.; Gülhan, A.; Esser, B.; *Determination of NO-Rotational and Vibrational Temperature Profiles in a High Enthalpy Flow Field with Nonequilibrium*, 1st Joint French-German Symp. of Simulation of Atmospheric Entries by Means of Ground Test Facilities, Stuttgart, 1999.

[7]   Del Veccio, A.; Palumbo, G.; Koch, U.; Gülhan, A.; *Temperature Measurements by Laser-induced Fluorescence Spectroscopy in Nonequilibrium High Enthalpy Flow*, Journal of Thermophysics and Heat Transfer, Vol. 14, No. 2, 2000.

[8]   Koch, U.; Esser, B.; Gülhan, A.; *Two Dimensional Spatially Resolved Two Photon Oxygen Atom Laser Induced Fluorescence Measurements in the Flow Field of the Arc Heated Facility L3K*, 5th European Symposium on Aerothermodynamics for Space Vehicles, Cologne, Germany, November 2004.

[9]   Gülhan, A.; Esser, B.; *A Study on Heat Flux Measurements in High Enthalpy Flows*, 35th AIAA Thermophysics Conference, Paper AIAA 2001-3011, Anaheim, CA, USA, June 2001.

[10] Gülhan, A.; Esser, B., Del Vecchio, A., Löhle, S., Sauvage, N., Chazot, O., Asma, C.O., *Comparative Heat Flux Measurements on Standard Models in Plasma Facilities*, AIAA/CIRA 13th International Space Planes and Hypersonic Systems and Technologies, Capua, Italy, May 2005.

[11] Vierkotten, B.; *Entwicklung und Verifikation eines kombinierten Hochtemperatur-Sensors für Druck, Temperatur und Wärmefluss*, Diplomarbeit, RWTH Aachen, 2011.

[12] Beck, J.V.; Blackwell, B.; St. Clair, C.R.; *Inverse Heat Conduction: Ill-posed Problems*, Wiley, New York, 1985.

[13] Playez, M., Asma, C., Verant, J.-L., Koch, U., Esser, B., Gülhan, A., *Calibration of facilities for CO_2 Validation Experiments in High Enthalpy and Plasmatron Facilities*, VKI CR 2007-33.